

# Robust Cosmological Bounds on Neutrinos and their Combination with Oscillation Results

**M. C. Gonzalez-Garcia**

*C.N. Yang Institute for Theoretical Physics  
State University of New York at Stony Brook  
Stony Brook, NY 11794-3840, USA,  
and: Institució Catalana de Recerca i Estudis Avançats (ICREA),  
Departament d'Estructura i Constituents de la Matèria and Institut de Ciències del  
Cosmos, Universitat de Barcelona, Diagonal 647, E-08028 Barcelona, Spain  
E-mail: concha@insti.physics.sunysb.edu*

**Michele Maltoni**

*Instituto de Física Teórica UAM/CSIC, Facultad de Ciencias, Universidad Autónoma  
de Madrid, Cantoblanco, E-28049 Madrid, Spain  
E-mail: michele.maltoni@uam.es*

**Jordi Salvado**

*Departament d'Estructura i Constituents de la Matèria and Institut de Ciències del  
Cosmos, Universitat de Barcelona, 647 Diagonal, E-08028 Barcelona, Spain  
E-mail: jsalvado@ecm.ub.es*

**ABSTRACT:** We perform a global analysis of cosmological observables in generalized cosmologies which depart from  $\Lambda$ CDM models by allowing non-vanishing curvature  $\Omega_k \neq 0$ , dark energy with equation of state with  $\omega \neq -1$ , the presence of additional relativistic degrees of freedom  $\Delta N_{\text{rel}}$ , and neutrino masses  $\Omega_\nu \neq 0$ . By combining the data from cosmic microwave background (CMB) experiments (in particular the latest results from WMAP-7), the present day Hubble constant ( $H_0$ ) measurement, the high-redshift Type-I supernovae (SN) results and the information from large scale structure (LSS) surveys, we determine the parameters in the 10-dimensional parameter space for such models. We present the results from the analysis when the full shape information from the LSS matter power spectrum (LSSPS) is included versus when only the corresponding distance measurement from the baryon acoustic oscillations (BAO) is accounted for. We compare the bounds on the neutrino mass scale in these generalized scenarios with those obtained for the 6+1 parameter analysis in  $\Lambda$ CDM +  $m_\nu$  models and we also study the dependence of those on the set of observables included in the analysis. Finally we combine these results with the information on neutrino mass differences and mixing from the global analysis of neutrino oscillation experiments and derive the presently allowed ranges for the two laboratory probes of the absolute scale of neutrino mass: the effective electron neutrino mass in single beta decay and the effective Majorana neutrino mass in neutrinoless  $\beta\beta$  decay.

---

## Contents

<b>1. Introduction</b>	<b>1</b>
<b>2. Cosmological Inputs and Data Analysis</b>	<b>4</b>
<b>3. Results of the Cosmological Fits</b>	<b>6</b>
<b>4. Combination with Oscillation Data</b>	<b>11</b>
<b>5. Summary</b>	<b>13</b>

---

## 1. Introduction

It is now an established fact that neutrinos are massive and leptonic flavors are not symmetries of Nature [1, 2]. In the last decade this picture has become fully proved thanks to the upcoming of a set of precise experiments. In particular, the results obtained with solar [3–12] and atmospheric neutrinos [13, 14] have been confirmed in experiments using terrestrial beams: neutrinos produced in nuclear reactors [15, 16] and accelerators [17–20] facilities have been detected at distances of the order of hundreds of kilometers [21].

The minimum joint description of all the neutrino data requires mixing among all the three known neutrinos ( $\nu_e$ ,  $\nu_\mu$ ,  $\nu_\tau$ ), which can be expressed as quantum superpositions of three massive states  $\nu_i$  ( $i = 1, 2, 3$ ) with masses  $m_i$ . This implies the presence of a leptonic mixing matrix in the weak charged current interactions [22, 23] which can be parametrized as:

$$U = \begin{pmatrix} 1 & 0 & 0 \\ 0 & c_{23} & s_{23} \\ 0 & -s_{23} & c_{23} \end{pmatrix} \cdot \begin{pmatrix} c_{13} & 0 & s_{13}e^{-i\delta_{\text{CP}}} \\ 0 & 1 & 0 \\ -s_{13}e^{i\delta_{\text{CP}}} & 0 & c_{13} \end{pmatrix} \cdot \begin{pmatrix} c_{21} & s_{12} & 0 \\ -s_{12} & c_{12} & 0 \\ 0 & 0 & 1 \end{pmatrix} \cdot \begin{pmatrix} e^{i\eta_1} & 0 & 0 \\ 0 & e^{i\eta_2} & 0 \\ 0 & 0 & 1 \end{pmatrix}, \quad (1.1)$$

where  $c_{ij} \equiv \cos \theta_{ij}$  and  $s_{ij} \equiv \sin \theta_{ij}$ . In addition to the Dirac-type phase  $\delta_{\text{CP}}$ , analogous to that of the quark sector, there are two physical phases  $\eta_i$  associated to the Majorana character of neutrinos and which are not relevant for neutrino oscillations [24, 25].

Given the observed hierarchy between the solar and atmospheric mass-squared splittings there are two possible non-equivalent orderings for the mass eigenvalues, which are conventionally chosen as

$$m_1 < m_2 < m_3 \quad \text{with} \quad \Delta m_{21}^2 \ll (\Delta m_{32}^2 \simeq \Delta m_{31}^2) \quad \text{with} \quad (\Delta m_{31}^2 > 0); \quad (1.2)$$

$$m_3 < m_1 < m_2 \quad \text{with} \quad \Delta m_{21}^2 \ll |\Delta m_{31}^2 \simeq \Delta m_{32}^2| \quad \text{with} \quad (\Delta m_{31}^2 < 0). \quad (1.3)$$

As it is customary we refer to the first option, Eq. (1.2), as the *normal* (N) scheme, and to the second one, Eq. (1.3), as the *inverted* (I) scheme; in this form they correspond to the two possible choices of the sign of  $\Delta m_{31}^2$ . In this convention the angles  $\theta_{ij}$  can be

taken without loss of generality to lie in the first quadrant,  $\theta_{ij} \in [0, \pi/2]$ , and the phases  $\delta_{CP}$ ,  $\eta_i \in [0, 2\pi]$ .

Within this context,  $\Delta m_{21}^2$ ,  $|\Delta m_{31}^2|$ ,  $\theta_{12}$ , and  $\theta_{23}$  are relatively well determined from oscillation experiments [26–29], while only an upper bound is derived for the mixing angle  $\theta_{13}$  and barely nothing is known on the phases and on the sign of  $\Delta m_{31}^2$ . Furthermore neutrino oscillation data provides as unique information on the absolute neutrino mass scale a lower bound

$$\sum m_i \gtrsim \sqrt{|\Delta m_{31}^2|} \quad \text{for N} \quad (1.4)$$

$$\sum m_i \gtrsim 2\sqrt{|\Delta m_{31}^2|} \quad \text{for I} \quad (1.5)$$

$$(1.6)$$

Conversely the neutrino mass scale is constrained in laboratory experiments searching for its kinematic effects in Tritium  $\beta$  decay which are sensitive to the so-called effective electron neutrino mass [30–32]

$$m_{\nu_e}^2 \equiv \sum_i m_i^2 |U_{ei}|^2 = c_{13}^2 c_{12}^2 m_1^2 + c_{13}^2 s_{12}^2 m_2^2 + s_{13}^2 m_3^2, \quad (1.7)$$

At present the most precise determination from the Mainz [33] and Troitsk [34] experiments give no indication in favor of  $m_{\nu_e} \neq 0$  and one sets an upper limit

$$m_{\nu_e} < 2.2 \text{ eV}, \quad (1.8)$$

at 95% confidence level (CL). A new experimental project, KATRIN [35], is under construction with an estimated sensitivity limit:  $m_{\nu_e} \sim 0.2 \text{ eV}$ .

Direct information on neutrino masses can also be obtained from neutrinoless double beta decay ( $0\nu\beta\beta$ ) searches provided they are Majorana particles. In the absence of other sources of lepton number violation in the low energy lagrangian, the  $0\nu\beta\beta$  decay amplitude is proportional to the effective Majorana mass of  $\nu_e$ ,  $m_{ee}$ ,

$$m_{ee} = \left| \sum_i m_i U_{ei}^2 \right| = \left| c_{13}^2 c_{12}^2 m_1 e^{i\eta_1} + c_{13}^2 s_{12}^2 m_2 e^{i\eta_2} + s_{13}^2 e^{-i\delta_{CP}} \right|, \quad (1.9)$$

which, in addition to the masses and mixing parameters that affect the tritium beta decay spectrum, depends also on the phases in the leptonic mixing matrix. The strongest bound from  $0\nu\beta\beta$  decay was imposed by the Heidelberg-Moscow group [36]

$$m_{ee} < 0.26 \text{ (0.34) eV} \quad \text{at 68\% (90\%) CL}, \quad (1.10)$$

which holds for a given prediction of the nuclear matrix element. However, there are large uncertainties in those predictions which may considerably weaken the bound [37]. A series of new experiments is planned with sensitivity of up to  $m_{ee} \sim 0.01 \text{ eV}$  [38].

Neutrinos, like any other particles, contribute to the total energy density of the Universe. Furthermore within what we presently know of their masses, the three Standard Model (SM) neutrinos are relativistic through most of the evolution of the Universe and they are very weakly interacting which means that they decoupled early in cosmic history. Depending on their exact masses they can impact the CMB spectra, in particular by altering the value of the redshift for matter-radiation equality. More importantly, their free

streaming suppresses the growth of structures on scales smaller than the horizon at the time when they become non-relativistic and therefore affects the matter power spectrum which is probed from surveys of the LSS distribution (see [39] for a detailed review of cosmological effects of neutrino mass).

Within their present precision, cosmological observations are sensitive to neutrinos only via their contribution to the energy density in our Universe,  $\Omega_\nu h^2$  (where  $h$  is the Hubble constant normalized to  $H_0 = 100 \text{ km s}^{-1} \text{ Mpc}^{-1}$ ).  $\Omega_\nu h^2$  is related to the total mass in the form of neutrinos

$$\Omega_\nu h^2 = \sum_i m_i / (94 \text{ eV}). \quad (1.11)$$

Therefore cosmological data mostly gives information on the sum of the neutrino masses and has very little to say on their mixing structure and on the ordering of the mass states (see Ref. [40] for a recent update on the sensitivity of future cosmological observations to the mass ordering.)

There is a growing literature on the information extracted from cosmological observations on the neutrino mass scale, starting with the analysis performed by the different experimental collaborations [41–45]. The basic observation is that, besides variations due to the observables considered, the bounds on the neutrino mass obtained depend on the assumptions made on the history of the cosmic expansion, or in other words, on how many parameters besides the  $\Lambda$ CDM model are allowed to vary when analyzing the cosmological data. Additionally depending on those assumptions some observables need or not to be considered in order to account for degeneracies among the parameters (for some recent analysis see [46–48]).

In this article we present the results of a global analysis of cosmological observables in  $\omega$ CDM +  $\Delta N_{\text{rel}} + m_\nu$  cosmologies which depart from  $\Lambda$ CDM models by allowing, besides neutrino masses  $\Omega_\nu \neq 0$ , non-vanishing curvature  $\Omega_k \neq 0$ , dark energy with equation of state with  $\omega \neq -1$  together with the presence of new particle physics whose effect on the present cosmological observations can be parametrized in terms of additional relativistic degrees of freedom  $\Delta N_{\text{rel}}$ . In particular this extends the most general analysis of Ref. [48] by accounting also for non-flatness effects. We adopt a purely phenomenological approach in analyzing the effect of a non-vanishing spatial curvature without addressing its origin. However it is worth mentioning that, within inflationary models which produce the simple initial conditions here considered it is difficult to end up with a significant  $\Omega_k$  [49]. We describe in Sec. 2 the different cosmological observables included in these 10-parameter analysis as well as our statistical treatment of those. The results of the analysis are presented in Sec. 3 where we discuss the differences obtained when the full shape information from the LSS matter power spectrum is included versus when only the corresponding distance measurement from the baryon acoustic oscillations is accounted for. We also compare the bounds on the neutrino mass scale in these  $\omega$ CDM +  $\Delta N_{\text{rel}} + m_\nu$  scenarios with those obtained for the 6+1 parameter analysis in  $\Lambda$ CDM +  $m_\nu$  models and we also study the dependence of those on the set of observables included in the analysis. These results are combined with the information on neutrino mass differences and mixing from the global analysis of neutrino oscillation experiments in Sec. 4 to derive the presently allowed ranges for the two laboratory probes of the absolute scale of neutrino mass: the effective neutrino mass in single beta decay  $m_{\nu_e}$  and the effective Majorana neutrino mass in neutrinoless  $\beta\beta$  decay  $m_{ee}$ . We summarize our conclusions in Sec. 5.

## 2. Cosmological Inputs and Data Analysis

Parameter	symbol
Hubble Constant	$H_0$
Baryon density	$\Omega_b h^2$
Dark matter density	$\Omega_c h^2$
Scalar spectral index	$n_s$
Optical Depth at Reionization	$\tau$
Amplitude of scalar power spectrum at $k = 0.05 \text{ Mpc}^{-1}$	$A_S$
Total neutrino mass	$\sum_{i=1,3} m_{\nu,i}$
Dark energy equation of state parameter	$\omega$
Effective number of extra relativistic degrees of freedom	$\Delta N_{\text{rel}}$
Spatial curvature density	$\Omega_k$

**Table 1:** Cosmological parameters used in our most general analysis.  $h = H_0/100$ . We denote the cosmology characterized by these parameters as  $\omega\text{CDM} + \Delta N_{\text{rel}} + m_\nu$ .

We consider cosmologies  $\omega\text{CDM} + \Delta N_{\text{rel}} + m_\nu$  characterized by the free parameters listed in Table 1. All parameters are as usually defined in the literature with the exception of  $\Delta N_{\text{rel}}$ . Our definition of extra relativistic degrees of freedom accounts for the fact that we have evidence of the existence of three and only three standard neutrino species which mix due to mass oscillations [21]. Their contribution to the energy budget of the universe is included in  $\Omega_\nu h^2$ .  $\Delta N_{\text{rel}}$  parametrizes the contribution of additional relativistic massless states of any spin to the radiation energy density. For convenience that contribution is normalized to the one from a spin 1/2 weakly interacting massless state. That normalization is  $\Delta N_{\text{rel}}$ .

In these cosmologies several parameter degeneracies appear in any of the cosmological observables. First, any experiment that measures the angular diameter or luminosity distance to a single redshift is not able to constrain  $\Omega_k$  because the distance depends not only on  $\Omega_k$ , but also on the expansion history of the universe. Thus for a universe containing matter and vacuum energy, one needs to combine at least two absolute distance indicators, or the expansion rates out to different redshifts to break this degeneracy. Furthermore when dark energy is dynamical,  $\omega \neq -1$ , a third distance indicator is required. Finally the presence of extra relativistic degrees of freedom  $\Delta N_{\text{rel}}$  changes the matter-radiation equality epoch, a change that can be compensated by the corresponding modification of the matter density  $\Omega_m h^2$ . As a result,  $\Delta N_{\text{rel}}$  and  $\Omega_m h^2$  are strongly degenerate unless a fourth distance indicator provides us with an independent constraint on  $\Omega_m h^2$ .

In our analysis we include the results from the 7-year data of WMAP [41] on the temperature and polarization anisotropies in the form of the temperature (TT), E-mode polarization (EE), B-mode polarization (BB), and temperature-polarization cross-correlation (TE) power spectra for which we use the likelihood function as provided by the collaboration<sup>1</sup>. A number of CMB experiments have probed smaller angular scales than WMAP. In particular we consider the results from the temperature power spectra from the Cosmic

<sup>1</sup>We notice that, although the models considered do not generate any B-mode polarization, in order to account for the information from EE and low-l TE data, the BB power spectrum must also be included in the analysis because WMAP provides the combined likelihood for the low-l TE, EE and BB spectra [50]

Background Imager (CBI) [51], the Very Small Array (VSA) [52], BOOMERANG [53] and the Arcminute Cosmology Bolometer Array Receiver (ACBAR), [54]. In order to avoid redundancies among the CMB data sets, we follow the procedure in Refs. [42, 55]. We use seven band powers for CBI (in the range  $948 < \ell < 1739$ ), five for VSA ( $894 < \ell < 1407$ ), seven for BOOMERANG ( $924 < \ell < 1370$ ), and sixteen band powers of ACBAR in the range  $900 < \ell < 2000$ . We do not include the results of the Background Imaging of Cosmic Extragalactic Polarization (BICEP) [56] experiment whose bands overlap excessively with WMAP and from QUaD [57] which observes the same region of sky as ACBAR and it is less precise [55]. Furthermore we do not include in the analysis the polarization results of these experiments. As mentioned above, in the analysis of WMAP we use the likelihood function as provided by the collaboration. For the other CMB experiments we build the corresponding likelihood functions from the data, covariance matrix and window functions given by each experiment. We compute theoretical CMB predictions using the fast Boltzmann code CAMB [58, 59]. Following the procedure outlined in Ref. [43] whenever it is required we account for the Sunyaev-Zel'dovich (SZ) effect by marginalizing over the amplitude of the SZ contribution parametrized by the model of Ref. [60]. We assume a uniform prior on the amplitude as  $0 < A_{\text{SZ}} < 2$ .

We also include the results from Ref. [61] on the present-day Hubble constant,  $H_0 = 74.2 \pm 3.6 \text{ km s}^{-1} \text{ Mpc}^{-1}$  where the quoted error includes both statistical and systematic errors. This measurement of  $H_0$  is obtained from the magnitude-redshift relation of 240 low- $z$  Type Ia supernovae at  $z < 0.1$ . We include this result as a Gaussian prior and neglect the slight cosmology dependence [47] of this constraint.

The results from luminosity measurements of high- $z$  Type Ia supernovae are included as presented in the compilation of the supernova data called the ‘‘Constitution’’ sample in Ref. [62] which consists of 397 supernovae and it is an extension of the ‘‘Union’’ sample [63]. With these data we build the corresponding likelihood function without including systematic errors whose precise values are still under debate [62]. In our analysis we marginalize over the absolute magnitude of the supernovae with a uniform prior.

Finally we also include the results from the matter power spectrum as derived from large scale structure surveys in two different forms. In one case we use the measurement of BAO scale obtained from the Two-Degree Field Galaxy Redshift Survey (2dFGRS) and the Sloan Digital Sky Survey Data Release 7 (SDSS DR7) [44]. In the other we include the full power spectrum of the SDSS DR7 survey [45] (which we label LSSPS).

For the analysis including the BAO scale, we use as input data the two distance ratios at  $z = 0.2$  and  $z = 0.35$  presented in Ref. [44] and build the corresponding likelihood function using the covariance matrix as given in that reference. As discussed in Ref. [44] the distance ratios can be considered as measurements of  $d_z \equiv rs(z_d)/D_V(z)$  and apply to any of the considered models.  $rs(z_d)$  is the comoving sound horizon at the baryon drag epoch and  $D_V(z) = [(1+z)^2 D_A^2 cz/H(z)]^{1/3}$  with  $D_A$  is the angular diameter distance and  $H(z)$  is the Hubble parameter. However in their fitting procedure the value of  $d_z$  is obtained by first assuming some fiducial cosmology, extracting the value of  $D_V(z)$  and then computing  $rs(z_d)/D_V(z)$  with  $rs(z_d)$  evaluated by that fiducial cosmology using the approximated formula of Eisenstein & Hu [64] for  $z_d$ . As discussed in Ref. [48] this approximated formula is not strictly valid for the extended cosmologies which we are considering. We correct for this effect by a) exactly evaluating the redshift at baryon drag epoch by using Eq.(B.5) in Ref. [48] in the extended cosmologies, and b) correcting for the use of the approximate formula in the presentation of the data by rescaling the predictions by a

factor  $r_s^{\text{fid}}(z_{d\text{ approx}})/r_s^{\text{fid}}(z_{d\text{ exact}})$  (we prefer to rescale the predictions since the covariance matrix is given for the data as presented).

In our second analysis we include the full SDSS DR7 data which consists of 45 bins, covering wavenumbers from  $k_{\text{min}} = 0.02 \text{ hMpc}^{-1}$  to  $k_{\text{max}} = 0.2 \text{ hMpc}^{-1}$  (where  $k_{\text{min}}$  and  $k_{\text{max}}$  denote the wavenumber at which the window functions of the first and last data point have their maximum). In this analysis we use the likelihood function as provided by the experiment. Together with the linear matter power spectrum it requires a smooth version of it with the baryon oscillations removed. We construct such no-wiggle spectrum for the extended cosmologies here considered from the linear matter power spectrum computed by CAMB using the method based on the discrete spectral analysis of the power spectrum described in Appendix A.1 of Ref. [48].

We also perform comparative analysis including only the  $\Lambda$ CDM parameters plus massive neutrinos (first seven in Table 1) fixing  $\omega = -1$   $\Delta N_{\text{rel}} = \Omega_k = 0$  for different combinations of the above observables.

Additional constraints on the cosmological parameters can be obtained if one includes in the analysis information on the growth of structure from other low redshift data. Among others the small scale primordial spectrum determined from Lyman-alpha forest clouds or the priors on the amplitude of mass fluctuations derived from different galaxy cluster samples. We have conservatively chosen not to include those in our analysis because generically these results are subject to model dependence assumptions which render them not directly applicable for the most general cosmologies here consider.

With the data from the different samples included in a given analysis and the theoretical predictions for them in terms of the relevant parameters  $\vec{x}$ , we construct the corresponding combined likelihood function. In Bayesian statistics our knowledge of  $\vec{x}$  is summarized by the posterior probability distribution function (p.d.f.)

$$p(\vec{x}|\mathcal{D}, \mathcal{P}) = \frac{\mathcal{L}(\mathcal{D}|\vec{x}) \pi(\vec{x}|\mathcal{P})}{\int \mathcal{L}(\mathcal{D}|\vec{x}') \pi(\vec{x}'|\mathcal{P}) d\vec{x}'} . \quad (2.1)$$

$\pi(\vec{x}|\mathcal{P})$  is the prior probability density for the parameters. In our analysis we assume a uniform prior probability for the  $\vec{x}$  parameters in Table 1. For  $\sum m_\nu$  and  $\Delta N_{\text{rel}}$  we imposed that they should be both  $\geq 0$ . Following standard techniques in order to reconstruct the posterior p.d.f. Eq. (2.1) we have developed a Markov Chain Monte Carlo (MCMC) generator which employs the Metropolis-Hasting algorithm including the adapting for the kernel function to increase the efficiency. Full details are given in Appendix B of Ref. [65]. For each combination of data we generate  $\mathcal{O}(50)$  chains in parallel and verify its convergence by studying the variation of the Gelman-Rubin  $R$ -parameter [66] imposing as convergence criteria  $R - 1 \lesssim 5 \times 10^{-2}$ .

### 3. Results of the Cosmological Fits

Our results for the two analysis in  $\omega$ CDM +  $\Delta N_{\text{rel}} + m_\nu$  cosmologies are presented in Figs. 1– 2 and in Table 2. In Fig. 1 we show the marginalized one-dimensional probability distributions for the ten independent parameters obtained from Eq.(2.1) as <sup>2</sup>

$$p_{1\text{-dim}}(x_i) = \int dx_{k \neq i} p(\vec{x}|\mathcal{D}, \mathcal{P}) . \quad (3.1)$$

---

<sup>2</sup>Technically this is obtained from the MCMC chain by discretizing the parameter space and counting the fraction of points in each cell.

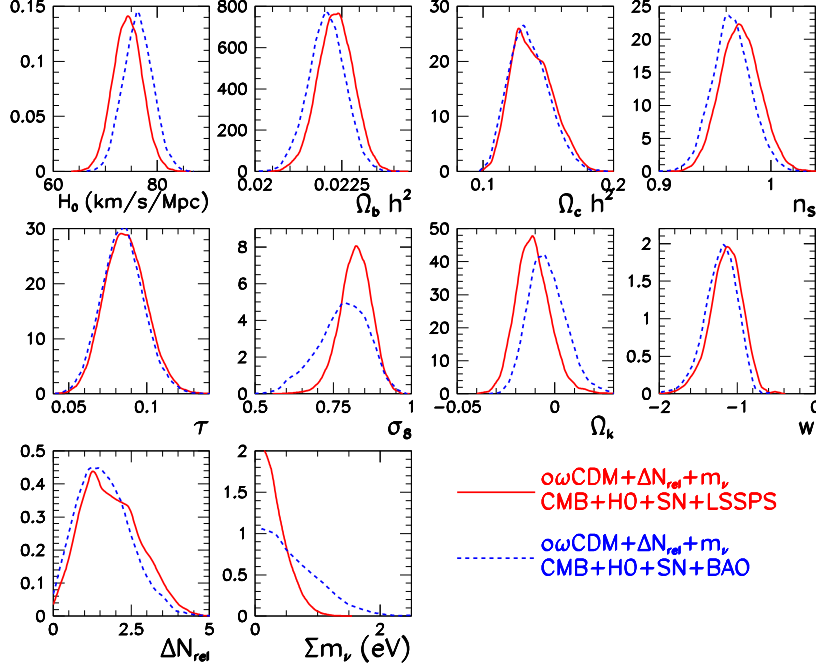


**Figure 1:** Constraints from our global analysis on the cosmological parameters of  $\omega\text{CDM} + \Delta N_{\text{rel}} + m_\nu$  for the analysis including CMB+H0+SN+LSSPS (solid red) and CMB+H0+SN+BAO (dotted blue). The different panels show the marginalized one-dimensional probability distributions for all parameters. For the neutrino mass see also Fig.3.

For convenience we show the information on the normalization of the scalar power spectrum in terms of the derived  $\sigma_8$  parameter which parametrizes the expected root mean square amplitude of the matter fluctuations in spheres of radius  $R = 8h^{-1}$  Mpc.

The best fit values given in the second and fourth columns in Table 2 are those for which  $p_{1-\text{dim}}(x_i^{\text{best}})$  is maximum. The allowed ranges at a given CL,  $x_{i,\text{min}}^{\text{CL}} \leq x_i \leq x_{i,\text{max}}^{\text{CL}}$ , are obtained from the condition

$$\text{CL} [x_{i,\text{min}}^{\text{CL}} \leq x_i \leq x_{i,\text{max}}^{\text{CL}}] = \int_{x_{i,\text{min}}^{\text{CL}}}^{x_{i,\text{max}}^{\text{CL}}} p_{1-\text{dim}}(x_i) \quad (3.2)$$

$$\text{with } p_{1-\text{dim}}(x_{i,\text{min}}^{\text{CL}}) = p_{1-\text{dim}}(x_{i,\text{max}}^{\text{CL}}) \quad (3.3)$$

$$\text{or } x_{i,\text{min}}^{\text{CL}} = 0 \quad \text{for } x_i = \Delta N_{\text{rel}}, \sum m_\nu \quad (3.4)$$

where (3.4) is used when there is no solution for condition (3.3).

Equivalently we define the marginalized two-dimensional probability distribution functions

$$p_{2-\text{dim}}(x_i, x_j) = \int dx_{k \neq i,j} p(\vec{x} | \mathcal{D}, \mathcal{P}), \quad (3.5)$$

and from these, we obtain the two-dimensional credibility regions with a given CL as the region with smallest area and with CL integral posterior probability. In practice they are obtained as the regions surrounded by a two-dimensional isoprobability contour which

	CMB+H0+SN+BAO			CMB+H0+SN+LSS-PS		
	best	1 $\sigma$	95% CL	best	1 $\sigma$	95% CL
$H_0$ km/s/Mpc	76.2	+3.0 -2.8	+5.7 -5.6	74.4	+2.8 -2.9	+5.6 -5.6
$\Omega_b h^2 \times 100$	2.205	+0.057 -0.050	+0.103 -0.105	2.239	+0.059 -0.046	+0.095 -0.108
$\Omega_c h^2$	0.131	+0.018 -0.013	+0.036 -0.023	0.128	+0.024 -0.009	+0.042 -0.018
$n_S$	0.961	+0.021 -0.015	+0.040 -0.030	0.971	+0.019 -0.017	+0.037 -0.033
$\tau$	0.086	+0.011 -0.015	+0.026 -0.028	0.083	+0.016 -0.011	+0.030 -0.023
$\sigma_8$	0.787	+0.091 -0.073	+0.135 -0.179	0.824	+0.051 -0.048	+0.097 -0.105
$\Omega_k$	-0.006	+0.010 -0.009	$-0.022 \leq \Omega_k \leq 0.016$	-0.011	+0.008 -0.009	$-0.028 \leq \Omega_k \leq 0.007$
$\omega$	-1.17	+0.19 -0.21	$-0.62 \leq \omega + 1 \leq 0.18$	-1.12	+0.21 -0.20	$-0.57 \leq \omega + 1 \leq 0.26$
$\Delta N_{\text{rel}}$	1.2	+1.1 -0.61	$0.08 \leq \Delta N_{\text{rel}} \leq 3.2$	1.3	+1.4 -0.54	$0.21 \leq \Delta N_{\text{rel}} \leq 3.6$
$\sum m_\nu$ (eV)		$\leq 0.77$	$\leq 1.5$		$\leq 0.37$	$\leq 0.76$

**Table 2:** Constraints from our global analysis for  $\omega\Lambda\text{CDM} + \Delta N_{\text{rel}} + m_\nu$  cosmologies. We show the values for the best fit parameters and the corresponding 1 $\sigma$  (68%) and 2 $\sigma$  (95%) allowed intervals.

contains the point of highest posterior probability and within which the integral posterior probability is CL. We plot in Fig.2 the 68% and 95% CL two-dimensional credibility regions for the last four parameters in Table 1. For the analysis including CMB+H0+SN+BAO (full regions) and including CMB+H0+SN+LSSPS (void regions).

Because of the degeneracies present in these cosmologies one finds, as expected, a degradation in the constraints of the *standard* parameters (ie those of the  $\Lambda\text{CDM}$  model) when compared with the analysis performed within the  $\Lambda\text{CDM}$  priors for the same set of observables (see for example table 1 in Ref. [41]). As seen in the figure this particularly affects the determination of  $\Omega_c$  (or equivalently  $\Omega_m$ ) as a consequence of the well-known degeneracy in the predictions of the CMB spectra between  $\Delta N_{\text{rel}}$  and  $\Omega_m$ . This is so because a simultaneous change of both can leave untouched the redshift for matter-radiation equality, which is well constrained by the ratio of height of the third and first peaks in the CMB spectra. This degeneracy is broken by the addition of the H0 prior as well as the independent determination of  $\Omega_m$  from the distance information from LSS, either using only BAO or the full power spectrum. It is interesting to notice that we find that data is better described by allowing a non-zero amount of extra radiation even though it is only at most a 2 $\sigma$  effect. This implies, for example, that models with extra light sterile neutrinos are favoured by the data (as discussed in Ref. [67] in the context of flat cosmologies with a cosmological constant) even for these  $\omega\Lambda\text{CDM}$  models. Most conservatively we can read the results as a 2 $\sigma$  upper bound on  $\Delta N_{\text{rel}} \leq 3.2$  (3.6) for the analysis including CMB+H0+SN+BAO (CMB+H0+SN+LSSPS).

We also find a widening in the allowed range of  $n_S$  as a consequence of its degeneracy with  $\Delta N_{\text{rel}}$  and with the dark energy equation of state  $\omega$ . Both change the ratio of generated power at low versus large angular scales in the CMB spectrum, an effect that can be offset by a change in the spectral index. Conversely we find that in these cosmologies  $\omega$  is considerably less constrained than in  $\omega\text{CDM}$  scenarios for which a 95% range  $-0.089 \leq$

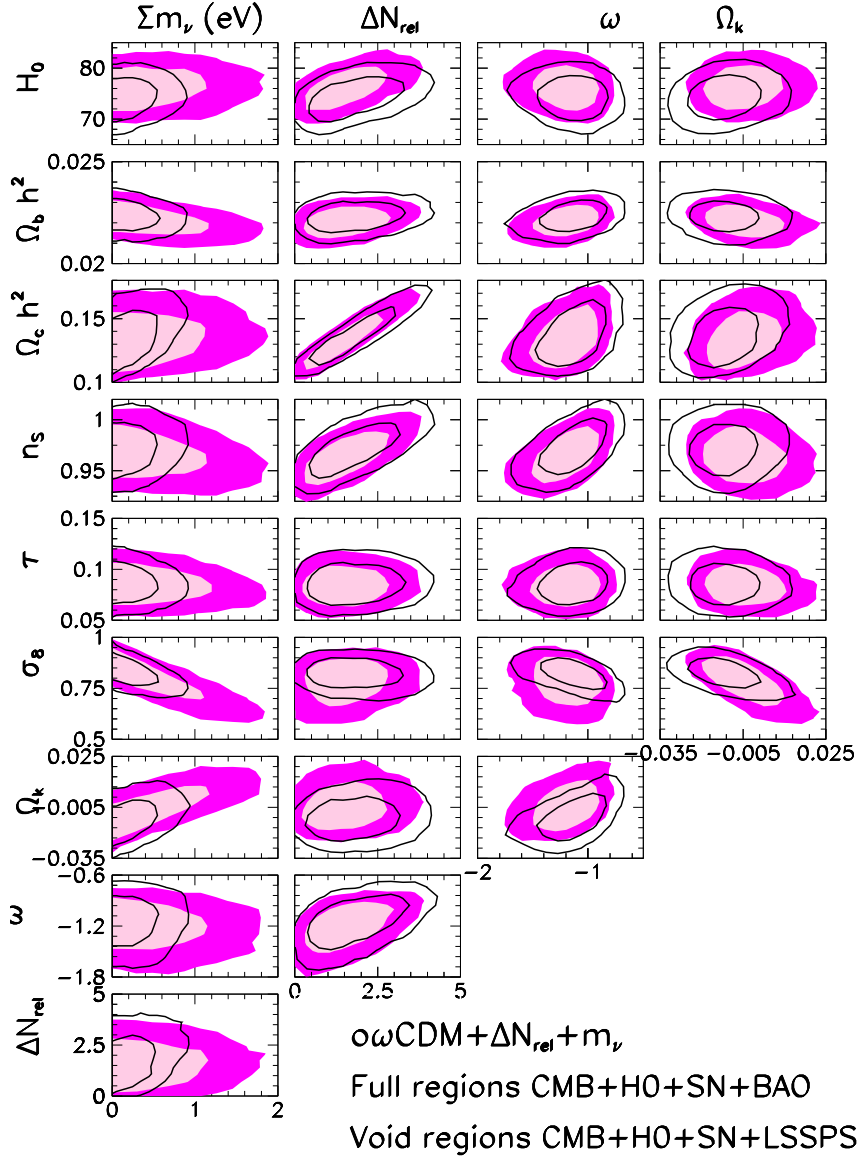


**Figure 2:** Constraints from our global analysis for  $\omega\Lambda\text{CDM} + \Delta N_{\text{rel}} + m_\nu$  cosmologies for the analysis including CMB+H0+SN+BAO (full regions) and for the analysis including CMB+H0+SN+LSSPS (void regions). We show the 68% and 95% CL two-dimensional credibility regions for the last four parameters in Table 1

$\omega + 1 \leq 0.12$  is obtained from the analysis of CMB+BAO+SN [41].

The normalization of the power spectrum as parametrized by  $\sigma_8$  is mostly affected by the presence of neutrino masses. Their main effect is to reduce the amplitude on the power spectrum on free-streaming scales therefore decreasing  $\sigma_8$ . There is also a residual degeneracy between  $\sigma_8$  and  $\Omega_k$  mostly associated with the fact that allowing for non-flat cosmologies permits to increase the amount of dark matter in the form of neutrinos without affecting  $\Omega_c$  and therefore minimizing their indirect impact on the CMB spectra. As a consequence we find that there is a correlation between the allowed range of neutrino

mass and  $\Omega_k$  as it is seen in the corresponding panel of Fig.2. This leads to a somewhat wider allowed range of  $\Omega_k$  when compared to the results obtained from the analysis of CMB+BAO+SN in  $\omega$ CDM scenarios  $-0.019 \leq \Omega_k \leq 0.0072$  [41].

Figures 1 and Fig.2 also display clearly the differences in the results obtained when the full shape information from the LSS matter power spectrum is included versus when only the corresponding distance measurement from BAO is accounted for. We see that, with the expected exception of the neutrino mass (and correspondingly of  $\sigma_8$ ), both sets of data lead to comparable precision on the determination of the cosmological parameters. Concerning the neutrino masses we find that neither of the two analysis show any evidence for neutrino mass and the best fit point is obtained for  $\sum m_\nu = 0$ . However the 95 % upper bound obtained when using BAO,  $\sum m_\nu \leq 1.5$ , is tighten by a about a factor 2,  $\sum m_\nu \leq 0.76$ , by considering instead the full LSSPS.

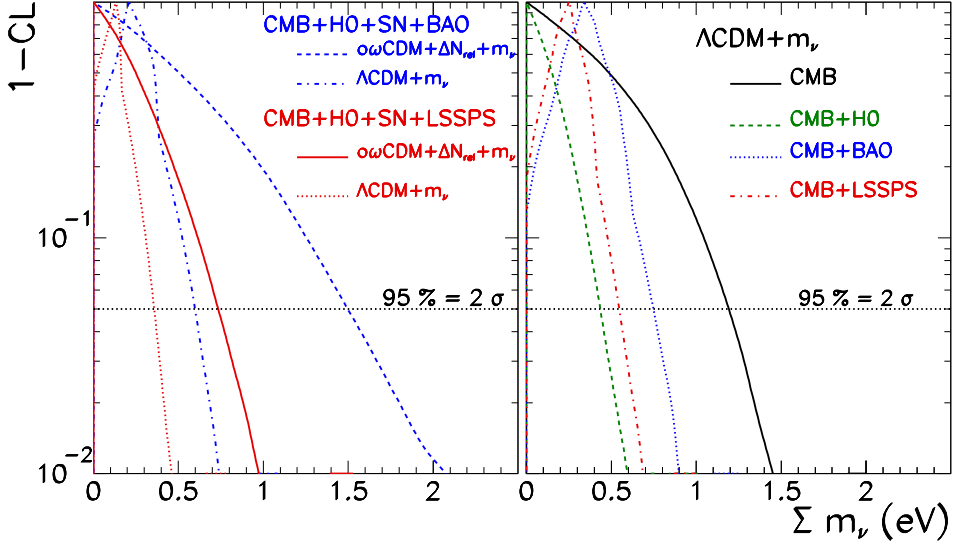


**Figure 3:** Constraint on  $\sum m_\nu$  as a function of the CL for the different analysis as labeled in the figure.

We plot in Fig.3 the bound on  $\sum m_\nu$  for the two analysis in the  $\omega$ CDM +  $\Delta N_{\text{rel}} + m_\nu$  cosmologies at a given CL together with the corresponding results from different analysis performed in the framework of  $\Lambda$ CDM +  $m_\nu$  models. The corresponding 95% CL bounds are listed in Table. 3. We find that for the same combination of observables CMB+H0+SN+BAO (CMB+H0+SN+LSSPS) the bound for a  $\Lambda$ CDM +  $m_\nu$  scenario is  $\sum m_\nu \leq 0.61$  ( $\sum m_\nu \leq 0.35$ ) which is a factor  $\sim 3$  (2) tighter than the corresponding one obtained in  $\omega$ CDM +  $\Delta N_{\text{rel}} + m_\nu$  cosmologies. However, we also find that at lower CL  $\Lambda$ CDM +  $m_\nu$  scenarios are better fitted with a non vanishing  $m_\nu$  when the information from CMB (and H0) is combined with the information from LSS surveys. This is, however, at most a  $1\sigma$  effect associated with the slight mismatches between the best fit values of the cosmological parameters obtained in the analysis of the observables in the context of the  $\Lambda$ CDM. This illustrates the well-known fact that overconstrained scenarios are more “sensitive” to small fluctuations in the data, due either to statistics or to an optimistic esti-

Model	Observables	$\Sigma m_\nu$ (eV) 95% Bound
$\omega\text{CDM} + \Delta N_{\text{rel}} + m_\nu$	CMB+H0+SN+BAO	$\leq 1.5$
$\omega\text{CDM} + \Delta N_{\text{rel}} + m_\nu$	CMB+H0+SN+LSSPS	$\leq 0.76$
$\Lambda\text{CDM} + m_\nu$	CMB+H0+SN+BAO	$\leq 0.61$
$\Lambda\text{CDM} + m_\nu$	CMB+H0+SN+LSSPS	$\leq 0.36$
$\Lambda\text{CDM} + m_\nu$	CMB (+SN)	$\leq 1.2$
$\Lambda\text{CDM} + m_\nu$	CMB+BAO	$\leq 0.75$
$\Lambda\text{CDM} + m_\nu$	CMB+LSSPS	$\leq 0.55$
$\Lambda\text{CDM} + m_\nu$	CMB+H0	$\leq 0.45$

**Table 3:** 95 % upper bound on the sum of the neutrino masses from the different cosmological analysis. The analysis within  $\Lambda\text{CDM} + m_\nu$  models including only CMB data or in combination with SN yield the same 95% bound.

mate of the systematic uncertainties. Consequently, even if more conservative, the bounds derived on more general scenarios are more robust against these effects.

#### 4. Combination with Oscillation Data

We present in this section the allowed ranges for the sum of the neutrino masses and the two laboratory probes of the absolute scale of neutrino mass: the effective neutrino mass in single beta decay  $m_{\nu_e}$  and the effective Majorana neutrino mass in neutrinoless  $\beta\beta$  decay  $m_{ee}$ , obtained from the combination of the cosmological analysis discussed above, with the information from the global analysis of solar, atmospheric, reactor and accelerator longbaseline (LBL) neutrino experiments in terms of flavour oscillations between the three neutrinos [26].

Our starting point is the  $\chi^2$  function from the oscillation analysis

$$\chi_{\text{O}}^2(\Delta m_{21}^2, \Delta m_{31}^2, \theta_{12}, \theta_{13}, \theta_{23}, \delta_{\text{CP}}) = \chi_{\text{Solar+KamLAND}}^2(\Delta m_{21}^2, \theta_{12}, \theta_{13}) + \chi_{\text{CHOOZ}}^2(\Delta m_{31}^2, \theta_{13}) + \chi_{\text{ATM+LBL}}^2(\Delta m_{21}^2, \Delta m_{31}^2, \theta_{12}, \theta_{13}, \theta_{23}, \delta_{\text{CP}}) \quad (4.1)$$

$$\Rightarrow \chi_{\text{O}}^2(m_{\nu_e}, m_{ee}, \sum m_{\nu_i}) \quad (4.2)$$

where the last step is obtained after marginalization over  $\Delta m_{31}^2$  and  $\theta_{23}$  and allowing for variation of the two phases  $\eta_1$  and  $\eta_2$  within their full range.

In Fig.4 we plot the 95% allowed regions (for 2 dof) in the planes  $(m_{\nu_e}, \sum m_\nu)$  and  $(m_{ee}, \sum m_\nu)$  as obtained from the marginalization of  $\chi_{\text{O}}^2(m_{\nu_e}, m_{ee}, \sum m_{\nu_i})$  with respect to the undisplayed parameter in each plot. In the figure we also show superimposed the single parameter 95% bounds on  $\sum m_{\nu_i}$  from the different cosmological analysis described in the previous section. The figure illustrates the well-known fact that currently for either mass ordering the results from neutrino oscillation experiments imply a lower bound on  $m_{\nu_e}$ . On the contrary  $m_{ee}$  is only bounded from below for the case of the normal ordering while full cancellation due to the unknown Majorana phases is still allowed for the inverted ordering.

In order to obtain the global combined ranges we first define a one parameter equivalent  $\chi_{\text{C}}^2(\sum m_\nu)$  function [68] for a given cosmological analysis from the condition that it leads to the same CL intervals than the corresponding marginalized one-dimensional probability distribution function:

$$\text{CL} = \frac{1}{2\pi} \int_0^{\chi_{\text{C}}^2(\sum m_\nu)} \frac{e^{-x^2/2}}{\sqrt{x}} \quad (4.3)$$

Model	Observables	Cosmo+Oscillations 95% Ranges		
		$m_{\nu_e}$ (eV)	$m_{ee}$ (eV)	$\Sigma m_\nu$ (eV)
$o\omega\text{CDM} + \Delta N_{\text{rel}} + m_\nu$	CMB+H0+SN+BAO	N [0.0047 – 0.51] I [0.047 – 0.51]	N [0.00 – 0.51] I [0.014 – 0.51]	N [0.056 – 1.5] I [0.098 – 1.5]
$o\omega\text{CDM} + \Delta N_{\text{rel}} + m_\nu$	CMB+H0+SN+LSSPS	N [0.0047 – 0.27] I [0.047 – 0.27]	N [0.00 – 0.25] I [0.014 – 0.25]	N [0.056 – 0.75] I [0.098 – 0.76]
$\Lambda\text{CDM} + m_\nu$	CMB+H0+SN+BAO	N [0.0047 – 0.20] I [0.048 – 0.21]	N [0.00 – 0.20] I [0.014 – 0.21]	N [0.056 – 0.61] I [0.097 – 0.61]
$\Lambda\text{CDM} + m_\nu$	CMB+H0+SN+LSSSP	N [0.0047 – 0.12] I [0.047 – 0.12]	N [0.00 – 0.12] I [0.014 – 0.12]	N [0.056 – 0.36] I [0.098 – 0.36]
$\Lambda\text{CDM} + m_\nu$	CMB (+SN)	N [0.0047 – 0.40] I [0.047 – 0.40]	N [0.00 – 0.40] I [0.014 – 0.41]	N [0.056 – 1.2] I [0.098 – 1.2]
$\Lambda\text{CDM} + m_\nu$	CMB+BAO	N [0.0052 – 0.25] I [0.047 – 0.25]	N [0.00 – 0.25] I [0.014 – 0.25]	N [0.056 – 0.75] I [0.099 – 0.75]
$\Lambda\text{CDM} + m_\nu$	CMB+LSSPS	N [0.0047 – 0.18] I [0.048 – 0.19]	N [0.00 – 0.18] I [0.014 – 0.19]	N [0.056 – 0.55] I [0.099 – 0.55]
$\Lambda\text{CDM} + m_\nu$	CMB+H0	N [0.0047 – 0.14] I [0.047 – 0.16]	N [0.00 – 0.14] I [0.014 – 0.16]	N [0.056 – 0.44] I [0.097 – 0.45]

**Table 4:** 95% allowed ranges for the different probes of the absolute neutrino mass scale from the global analysis of the cosmological data with the results from oscillation experiments. The analysis within  $\Lambda\text{CDM} + m_\nu$  models including only CMB data or in combination with SN yield the same 95% ranges.

where CL is obtained from Eq. (3.2) with  $\sum m_{\nu_i} = x_{i,\text{max}}^{\text{CL}}$  and  $x_{i,\text{min}}^{\text{CL}} = 0$  when the lower bound for that CL is 0 (which implies that the function  $\chi_C^2(\sum m_\nu)$  is single valued). When  $x_{i,\text{min}}^{\text{CL}} \neq 0$  the function  $\chi_C^2(\sum m_\nu)$  takes the same value for  $\sum m_{\nu_i} = x_{i,\text{max}}^{\text{CL}}$  and  $\sum m_{\nu_i} = x_{i,\text{min}}^{\text{CL}}$ .

Finally we construct

$$\chi_{\text{O+C}}^2(m_{\nu_e}, m_{ee}, \sum m_{\nu_i}) = \chi_{\text{O}}^2(m_{\nu_e}, m_{ee}, \sum m_{\nu_i}) + \chi_{\text{C}}^2(\sum m_\nu), \quad (4.4)$$

from which we obtain the the  $2\sigma$  1-dim allowed ranges for  $m_{\nu_e}$ ,  $m_{ee}$ , and  $\sum m_{\nu_i}$  given in Table 4 from the condition

$$\Delta\chi_{\text{O+C}}^2(m_{\nu_e}) = \text{Min}_{(m_{ee}, \sum m_{\nu_i})} \left[ \chi_{\text{O+C}}^2(m_{\nu_e}, m_{ee}, \sum m_{\nu_i}) \right] - \chi_{\text{O+C,min}}^2 < 4, \quad (4.5)$$

and equivalently for  $m_{ee}$  and  $\sum m_{\nu_i}$ .

The results show that, even for the most restrictive analysis including LSSPS, part of the allowed ranges for  $m_{\nu_e}$  in the context of the  $o\omega\text{CDM} + \Delta N_{\text{rel}} + m_\nu$  cosmologies are within the reach of the KATRIN experiment. On the contrary this is not the case for  $\Lambda\text{CDM} + m_\nu$  models unless only the information of CMB and BAO (or SN) is included. We

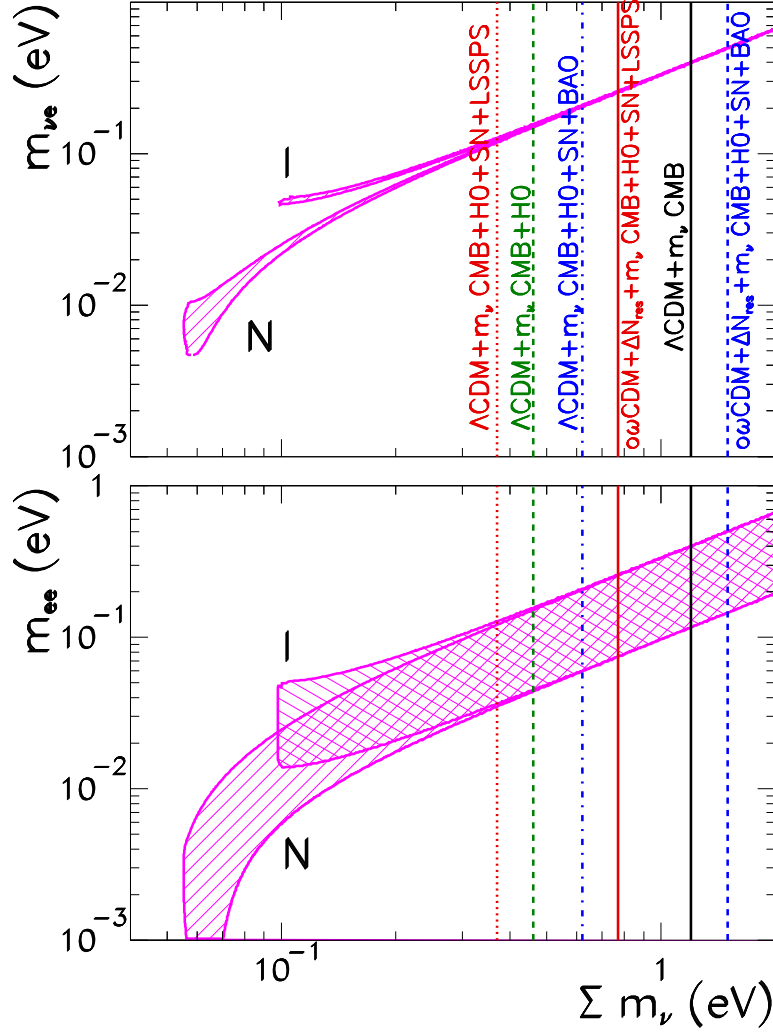


**Figure 4:** 95% allowed regions (for 2 dof) in the planes  $(m_{\nu e}, \sum m_\nu)$  and  $(m_{ee}, \sum m_\nu)$  from the global analysis of oscillation data (full regions). We also show superimposed the 95% upper bounds on  $\sum m_\nu$  from cosmological constraints for the different analysis as labeled in the figure.

also find that near future neutrinoless double beta decay can test some of the allowed ranges in all these scenarios. This will be complementary to the improvement on the expected sensitivity from upcoming cosmological probes such as the Planck mission [69].

## 5. Summary

In this work we have studied the information on the absolute value of the neutrino mass which can be obtained from the analysis of the cosmological data in  $\omega\Lambda\text{CDM} + \Delta N_{\text{rel}} + m_\nu$  cosmologies in which besides neutrino masses, one allows for non-vanishing curvature, dark energy with equation of state with  $\omega \neq -1$  together with the presence of new particle physics whose effect on the present cosmological observations can be parametrized in terms of additional relativistic degrees of freedom. To break the degeneracies in these models,

at least the information from four different cosmological probes must be combined. Thus we have performed analysis including the data from CMB experiments, the present day Hubble constant  $H_0$ , measurement, the high-redshift Type-I SN results and the information from large scale LSS surveys. We have compared the results from the analysis when the full shape information from the LSS matter power spectrum is included versus when only the corresponding distance measurement from the baryon acoustic oscillations is consider.

Our results are summarize in Table 2. Because of the degeneracies present in these cosmologies one finds a degradation in the constraints of the *standard* parameters (ie those of the  $\Lambda$ CDM model) when compared with the analysis performed within the  $\Lambda$ CDM priors for the same set of observables. Concerning the neutrino masses we find that neither of the two analysis show any evidence for neutrino mass and the best fit is obtained for  $\sum m_\nu = 0$ . However the 95 % upper bound obtained when using BAO,  $\sum m_\nu \leq 1.5$ , is tighten by a about a factor 2,  $\sum m_\nu \leq 0.76$ , by considering instead the full LSSPS. We have compared these results with those obtained from different analysis performed in the framework of  $\Lambda$ CDM+ $m_\nu$  models. The corresponding 95% CL bounds are listed in Table. 3. We find that for the same combination of observables CMB+HO+SN+BAO (CMB+HO+SN+LSSPS) the bound for a  $\Lambda$ CDM +  $m_\nu$  scenario is  $\sum m_\nu \leq 0.61$  ( $\sum m_\nu \leq 0.35$ ) which is a factor  $\sim 3$  (2) tighter than the corresponding one obtained in  $\omega$ CDM +  $\Delta N_{\text{rel}}$  +  $m_\nu$  cosmologies.

Finally we have statistically combined these results with the information on neutrino mass differences and mixing from the global analysis of neutrino oscillation experiments and we have derived the presently allowed ranges for the two laboratory probes of the absolute scale of neutrino mass: the effective neutrino mass in single beta decay  $m_{\nu_e}$  and the effective Majorana neutrino mass in neutrinoless  $\beta\beta$  decay  $m_{ee}$ . These results can be used to directly address the capabilities of the future  $\beta$  and neutrinoless- $\beta\beta$  decay experiments to probe the allowed parameter space.

## Acknowledgments

We are specially indebted to J. Taron for his collaboration in the early stages of this project and comments on the final version. We thank R. Jimenez, E. Nardi and L. Verde for comments. This work is supported by Spanish MICINN grants 2007-66665-C02-01, FPA-2009-08958 and FPA-2009-09017 and consolider-ingenio 2010 grant CSD-2008-0037, by CSIC grant 200950I111, by CUR Generalitat de Catalunya grant 2009SGR502, by Comunidad Autonoma de Madrid through the HEPHACOS project P-ESP-00346, by USA-NSF grant PHY-0653342 and by EU grant EURONU.

## References

- [1] B. Pontecorvo, *Neutrino experiments and the question of leptonic-charge conservation*, *Sov. Phys. JETP* **26** (1968) 984–988.
- [2] V. N. Gribov and B. Pontecorvo, *Neutrino astronomy and lepton charge*, *Phys. Lett.* **B28** (1969) 493.
- [3] B. T. Cleveland *et al.*, *Measurement of the solar electron neutrino flux with the Homestake chlorine detector*, *Astrophys. J.* **496** (1998) 505–526.
- [4] F. Kaether, W. Hampel, G. Heusser, J. Kiko, and T. Kirsten, *Reanalysis of the GALLEX solar neutrino flux and source experiments*, [arXiv:1001.2731](https://arxiv.org/abs/1001.2731).

- [5] **SAGE** Collaboration, J. N. Abdurashitov *et al.*, *Measurement of the solar neutrino capture rate with gallium metal. III: Results for the 2002–2007 data-taking period*, *Phys. Rev.* **C80** (2009) 015807, [[arXiv:0901.2200](#)].
- [6] **Super-Kamioke** Collaboration, J. Hosaka *et al.*, *Solar neutrino measurements in Super-Kamioke-I*, *Phys. Rev.* **D73** (2006) 112001, [[hep-ex/0508053](#)].
- [7] **SNO** Collaboration, B. Aharmim *et al.*, *Measurement of the  $\nu_e$  and total B-8 solar neutrino fluxes with the Sudbury Neutrino Observatory phase I data set*, *Phys. Rev.* **C75** (2007) 045502, [[nucl-ex/0610020](#)].
- [8] **SNO** Collaboration, B. Aharmim *et al.*, *Electron energy spectra, fluxes, and day-night asymmetries of B-8 solar neutrinos from the 391-day salt phase SNO data set*, *Phys. Rev.* **C72** (2005) 055502, [[nucl-ex/0502021](#)].
- [9] **SNO** Collaboration, B. Aharmim *et al.*, *An Independent Measurement of the Total Active 8B Solar Neutrino Flux Using an Array of  $^3\text{He}$  Proportional Counters at the Sudbury Neutrino Observatory*, *Phys. Rev. Lett.* **101** (2008) 111301, [[arXiv:0806.0989](#)].
- [10] **SNO** Collaboration, B. Aharmim *et al.*, *Low Energy Threshold Analysis of the Phase I and Phase II Data Sets of the Sudbury Neutrino Observatory*, [arXiv:0910.2984](#).
- [11] **Borexino** Collaboration, C. Arpesella *et al.*, *Direct Measurement of the Be-7 Solar Neutrino Flux with 192 Days of Borexino Data*, *Phys. Rev. Lett.* **101** (2008) 091302, [[arXiv:0805.3843](#)].
- [12] **Borexino** Collaboration, G. Bellini *et al.*, *Measurement of the solar 8B neutrino flux with 246 live days of Borexino and observation of the MSW vacuum-matter transition*, [arXiv:0808.2868](#).
- [13] **Super-Kamiokande** Collaboration, Y. Ashie *et al.*, *A Measurement of Atmospheric Neutrino Oscillation Parameters by Super-Kamiokande I*, *Phys. Rev.* **D71** (2005) 112005, [[hep-ex/0501064](#)].
- [14] **Kamiokande** Collaboration, S.-. R. Wendell *et al.*, *Atmospheric neutrino oscillation analysis with sub-leading effects in Super-Kamiokande I, II, and III*, [arXiv:1002.3471](#).
- [15] **KamLAND** Collaboration, I. Shimizu, *KamLAND (anti-neutrino status)*, *J. Phys. Conf. Ser.* **120** (2008) 052022.
- [16] **CHOOZ** Collaboration, M. Apollonio *et al.*, *Limits on Neutrino Oscillations from the CHOOZ Experiment*, *Phys. Lett.* **B466** (1999) 415–430, [[hep-ex/9907037](#)].
- [17] **K2K** Collaboration, M. H. Ahn *et al.*, *Measurement of Neutrino Oscillation by the K2K Experiment*, *Phys. Rev.* **D74** (2006) 072003, [[hep-ex/0606032](#)].
- [18] **MINOS** Collaboration, P. Adamson *et al.*, *Measurement of Neutrino Oscillations with the MINOS Detectors in the NuMI Beam*, *Phys. Rev. Lett.* **101** (2008) 131802, [[arXiv:0806.2237](#)]; the most up-to-date results can be found in <http://www.numi.fnal.gov/PublicInfo/forscientists.html>
- [19] **MINOS** Collaboration, P. Adamson *et al.*, *New constraints on muon-neutrino to electron-neutrino transitions in MINOS*, [arXiv:1006.0996](#).
- [20] **MINOS** Collaboration, P. Adamson *et al.*, *Search for muon-neutrino to electron-neutrino transitions in MINOS*, *Phys. Rev. Lett.* **103** (2009) 261802, [[arXiv:0909.4996](#)].
- [21] M. C. Gonzalez-Garcia and M. Maltoni, *Phenomenology with Massive Neutrinos*, *Phys. Rept.* **460** (2008) 1–129, [[arXiv:0704.1800](#)].
- [22] Z. Maki, M. Nakagawa, and S. Sakata, *Remarks on the unified model of elementary particles*, *Prog. Theor. Phys.* **28** (1962) 870–880.

- [23] M. Kobayashi and T. Maskawa, *CP Violation in the Renormalizable Theory of Weak Interaction*, *Prog. Theor. Phys.* **49** (1973) 652–657.
- [24] S. M. Bilenky, J. Hosek, and S. T. Petcov, *On Oscillations of Neutrinos with Dirac and Majorana Masses*, *Phys. Lett.* **B94** (1980) 495.
- [25] P. Langacker, S. T. Petcov, G. Steigman, and S. Toshev, *On the Mikheev-Smirnov-Wolfenstein (MSW) Mechanism of Amplification of Neutrino Oscillations in Matter*, *Nucl. Phys.* **B282** (1987) 589.
- [26] M. C. Gonzalez-Garcia, M. Maltoni and J. Salvado, *Updated global fit to three neutrino mixing: status of the hints of theta13* *JHEP* **1004** (2010) 056 [[arXiv:1001.4524](#)].
- [27] G. L. Fogli, E. Lisi, A. Marrone, A. Palazzo, and A. M. Rotunno, *Neutrino masses and mixing: 2008 status*, *Nucl. Phys. Proc. Suppl.* **188** (2009) 27–30.
- [28] T. Schwetz, M. A. Tortola, and J. W. F. Valle, *Three-flavour neutrino oscillation update*, *New J. Phys.* **10** (2008) 113011, [[arXiv:0808.2016](#)].
- [29] M. Maltoni and T. Schwetz, *Three-flavour neutrino oscillation update and comments on possible hints for a non-zero  $\theta_{13}$* , [arXiv:0812.3161](#).
- [30] R. E. Shrock, *New Tests For, And Bounds On, Neutrino Masses And Lepton Mixing*, *Phys. Lett. B* **96** (1980) 159.
- [31] F. Vissani, *Non-oscillation searches of neutrino mass in the age of oscillations* *Nucl. Phys. Proc. Suppl.* **100** (2001) 273 [[hep-ph/0012018](#)].
- [32] Y. Farzan, O. L. G. Peres and A. Y. Smirnov, *Neutrino mass spectrum and future beta decay experiments*, *Nucl. Phys. B* **612** (2001) 59 [[hep-ph/0105105](#)].
- [33] J. Bonn *et al.*, *the Mainz neutrino mass experiment*, *Nucl. Phys. Proc. Suppl.* **91** (2001) 273.
- [34] V. M. Lobashev *et al.*, *Direct search for neutrino mass and anomaly in the tritium beta-spectrum: Status of Troitsk neutrino mass experiment* *Nucl. Phys. Proc. Suppl.* **91** (2001) 280.
- [35] **KATRIN** Collaboration, A. Osipowicz *et al.* *KATRIN: A next generation tritium beta decay experiment with sub-eV sensitivity for the electron neutrino mass*, [hep-ex/0109033](#).
- [36] H. V. Klapdor-Kleingrothaus *et al.*, *Latest results from the Heidelberg-Moscow double-beta-decay experiment*, *Eur. Phys. J. A* **12** (2001) 147, [[hep-ph/0103062](#)].
- [37] P. Vogel, *Neutrinoless double beta decay*, [[hep-ph/0611243](#)].
- [38] F. T. . Avignone, S. R. Elliott and J. Engel, *Double Beta Decay, Majorana Neutrinos, and Neutrino Mass*, *Rev. Mod. Phys.* **80** (2008) 481 [[arXiv:0708.1033](#)].
- [39] J. Lesgourgues and S. Pastor, *Massive neutrinos and cosmology*, *Phys. Rept.* **429** (2006) 307, [[astro-ph/0603494](#)].
- [40] R. Jimenez, T. Kitching, C. Pena-Garay and L. Verde, *Can we measure the neutrino mass hierarchy in the sky?*, *JCAP* **1005** (2010) 035, [[arXiv:1003.5918](#)].
- [41] **WMAP** Collaboration, E. Komatsu, *et al.*, *Seven-Year Wilkinson Microwave Anisotropy Probe (WMAP) Observations: Cosmological Interpretation*, [[arXiv:1001.4538](#)].
- [42] **WMAP** Collaboration, J. Dunkley *et al.* *Five-Year Wilkinson Microwave Anisotropy Probe (WMAP) Observations: Likelihoods and Parameters from the WMAP data*, *Astrophys. J. Suppl.* **180**, 306 (2009), [[arXiv:0803.0586](#)].
- [43] **WMAP** Collaboration, D. N. Spergel *et al.* *Wilkinson Microwave Anisotropy Probe (WMAP) three year results: Implications for cosmology*, *Astrophys. J. Suppl.* **170**, 377 (2007), [[astro-ph/0603449](#)].

- [44] W. J. Percival *et al.*, *Baryon Acoustic Oscillations in the Sloan Digital Sky Survey Data Release 7 Galaxy Sample*, *Mon. Not. Roy. Astron. Soc.* **401** (2010) 2148, [[arXiv:0907.1660](#)].
- [45] B. A. Reid *et al.*, *Cosmological Constraints from the Clustering of the Sloan Digital Sky Survey DR7 Luminous Red Galaxies*, *Mon. Not. Roy. Astron. Soc.* **404** (2010) 60, [[arXiv:0907.1659](#)].
- [46] S. Hannestad, A. Mirizzi, G. G. Raffelt and Y. Y. Y. Wong, *Neutrino and axion hot dark matter bounds after WMAP-7*, [arXiv:1004.0695](#).
- [47] B. A. Reid, L. Verde, R. Jimenez and O. Mena, *Robust Neutrino Constraints by Combining Low Redshift Observations with the CMB*, *JCAP* **1001**, 003 (2010) [[arXiv:0910.0008](#)].
- [48] J. Hamann, S. Hannestad, J. Lesgourgues, C. Rampf and Y. Y. Y. Wong, *Cosmological parameters from large scale structure - geometric versus shapeinformation*, 1003.3999.
- [49] D. H. Lyth and A. Riotto, *Particle physics models of inflation and the cosmological density perturbation*, *Phys. Rept.* **314** (1999) 1 [[hep-ph/98072278](#)] and references therein.
- [50] **WMAP** Collaboration, D. Larson, *et al.*, *Seven-Year Wilkinson Microwave Anisotropy Probe (WMAP) Observations: Power Spectra and WMAP-Derived Parameters*, [[arXiv:1001.4635](#)].
- [51] A. C. S. Readhead *et al.*, *Extended Mosaic Observations with the Cosmic Background Imager*, *Astrophys. J.* **609** (2004) 498, [[astro-ph/0402359](#)].
- [52] C. Dickinson *et al.*, *High sensitivity measurements of the CMB power spectrum with the extended Very Small Array*, *Mon. Not. Roy. Astron. Soc.* **353** (2004) 732, [[astro-ph/0402498](#)].
- [53] J. E. Ruhl *et al.*, *Improved measurement of the angular power spectrum of temperature anisotropy in the CMB from two new analyses of BOOMERANG observations*, *Astrophys. J.* **599** (2003) 786, [[astro-ph/0212229](#)].
- [54] C. L. Reichardt *et al.*, *High resolution CMB power spectrum from the complete ACBAR data set*, *Astrophys. J.* **694** (2009) 1200, [[arXiv:0801.1491](#)].
- [55] F. Finelli, J. Hamann, S. M. Leach and J. Lesgourgues, *Single-field inflation constraints from CMB and SDSS data*, *JCAP* **1004**, 011 (2010), [[arXiv:0912.0522](#)].
- [56] H. C. Chiang *et al.*, *Measurement of CMB Polarization Power Spectra from Two Years of BICEP Data*, *Astrophys. J.* **711** (2010) 1123, [[arXiv:0906.1181](#)].
- [57] **QUaD** Collaboration, M. L. Brown *et al.*, *Improved measurements of the temperature and polarization of the CMB from QUaD*, *Astrophys. J.* **705** (2009) 978, [[arXiv:0906.1003](#)].
- [58] A. Lewis, A. Challinor and A. Lasenby, *Efficient Computation of CMB anisotropies in closed FRW models*, *Astrophys. J.* **538** (2000) 473, [[astro-ph/9911177](#)].
- [59] U. Seljak and M. Zaldarriaga, *A Line of Sight Approach to Cosmic Microwave Background Anisotropies*, *Astrophys. J.* **469** (1996) 437, [[astro-ph/9603033](#)]; M. Zaldarriaga and U. Seljak, *CMBFAST for spatially closed universes*, *Astrophys. J. Suppl.* **129** (2000) 431, [[astro-ph/9911219](#)].
- [60] E. Komatsu and U. Seljak, *The Sunyaev-Zel'dovich angular power spectrum as a probe of cosmological parameters*, *Mon. Not. Roy. Astron. Soc.* **336**, 1256 (2002), [[astro-ph/0205468](#)].
- [61] A. G. Riess *et al.*, *A Redetermination of the Hubble Constant with the Hubble Space Telescope from a Differential Distance Ladder*, *Astrophys. J.* **699**, 539 (2009), [[arXiv:0905.0695](#)].
- [62] M. Hicken *et al.*, *Improved Dark Energy Constraints from 100 New CfA Supernova Type Ia Light Curves* *Astrophys. J.* **700** (2009) 1097, [[arXiv:0901.4804](#)].

- [63] **Supernova Cosmology Project** Collaboration, M. Kowalski *et al.* *Improved Cosmological Constraints from New, Old and Combined Supernova Datasets*, *Astrophys. J.* **686**, 749 (2008), [[arXiv:0804.4142](#)].
- [64] D. J. Eisenstein and W. Hu, *Baryonic Features in the Matter Transfer Function*, *Astrophys. J.* **496** (1998) 605, [[astro-ph/9709112](#)].
- [65] M. C. Gonzalez-Garcia, M. Maltoni and J. Salvado, *Direct determination of the solar neutrino fluxes from solar neutrino data*, *JHEP* **1005** (2010) 072, [[arXiv:0910.4584](#)].
- [66] A. Gelman and D. B. Rubin, *Inference from iterative simulation using multiple sequences*, *Statistical Science* **7** (1992) 457.
- [67] J. Hamann, S. Hannestad, G. G. Raffelt, I. Tamborra and Y. Y. Y. Wong, *Cosmology seeking friendship with sterile neutrinos*, [[arXiv:1006.5276](#)].
- [68] G. L. Fogli *et al.*, *Observables sensitive to absolute neutrino masses (Addendum)*, *Phys. Rev. D* **78** (2008) 033010, [[arXiv:0805.2517](#)]; *Observables sensitive to absolute neutrino masses: A reappraisal after WMAP-3y and first MINOS results*, *Phys. Rev. D* **75** (2007) 053001 [[hep-ph/0608060](#)]; *Observables sensitive to absolute neutrino masses: Constraints and correlations from world neutrino data*, *Phys. Rev. D* **70** (2004) 113003, [[hep-ph/0408045](#)].
- [69] **Planck** Collaboration, *Planck: The scientific programme*, [[astro-ph/0604069](#)].